Indian Journal of Pure & Applied Physics
Vol. 45, September 2007, pp. 749-753

Dielectric study of spin coated nano-thick $BaZr_xTi_{1-x}O_3$ film

S K Rout[1], T Badapanda & S Panigrahi

Department of Physics, National Institute of Technology, Rourkela

Received 2 August 2006; revised 14 February 2007; accepted 3 July 2007

Barium zirconium titanate thin films are attractive candidates for dynamic random access memories and tunable microwave devices. Barium zirconate titanate $Ba(Zr_xTi_{1-x})\ O_3$ (BZT, y = 0.0, 0.2, 0.4) ceramics have been prepared by a sol-gel process. X-ray diffraction studies confirmed that the films of BZT are in crystalline form and of single phase. The SEM study shows that the films of homogeneous microstructure and Zr content strongly influence the grain size of the film. The grain size decreased and the microstructure became dense when Zr was substituted for Ti. The room temperature dielectric study shows that the permittivity as well as dielectric loss tangent decreases with increase in Zr content in the film. The *ac* conductivity was evaluated from dielectric data and was found to be decrease with increase in Zr concentration.

Keywords*:* Perovskite, Dielectrics, Thin film, $BaTiO_3$-$BaZrO_3$, Grain size
IPC Code: G01R27/26

1 Introduction

Barium strontium titanate (Ba,Sr) TiO_3(BST) is a high-k (dielectric constant) material which is commonly used to replace silicon dioxide (SiO_2) as the dielectric in advance memory devices. The high dielectric constant combined with a low dissipation factor makes BST one of the promising candidates for dynamic random access memory (DRAM) applications. $BaTiO_3$ is known to have a large electromechanical coupling factor. The interest in high strain piezoelectric materials is increasing for electromechanical transducers and various related applications[1-3]. Though the large families of lead-based perovskites are practically used such as dielectrics for capacitors, actuators and relaxors, etc, Lead –free compositions have attracted interest because of their obvious environmental friendly applications. Recently, Ba $(Ti_{1-x}\ Zr_x)\ O_3$ (BTZ) has been chosen as an alternative to BST in the fabrication of ceramic capacitors[4-7] because Zr^{+4} is chemically more stable than Ti^{+4}. The solid solution of Barium titanate ($BaTiO_3$) and barium zirconate ($BaZrO_3$) ie Ba $(Ti_{1-x}\ Zr_x)\ O_3$ shows great similarity to the BST solid solution[8,9]. Substitution of Ti^{4+} (atomic weight of 47.9, ionic radius of 74.5 pm) with Zr^{4+} (atomic weight of 91.2, atomic radius of 86 pm) exhibits several interesting features in the dielectric behaviour of $BaTiO_3$ ceramics. When the Zr content is less than 10 at %, the BZT ceramics show normal ferroelectric behaviour and the dielectric anomalies corresponding to the cubic to tetragonal (T_c), tetragonal to orthorhombic (T_2), and orthorhombic to rhombohedral (T_3) phases have been clearly observed. At around 27 at %, Zr-concentration BZT ceramics exhibit typical diffuse paraelectric to ferroelectric phase transition behaviour in which T_c shifts to higher temperature with increase in frequency[10], which is caused by the inhomogeneous distribution of Zr ions on Ti sites and mechanical stress in the grain[6]. Again with increase of Zr ($\geq$ 0:42 at %) content the BZT materials exhibit like normal ferroelectric behaviour.

In this work, lead free Ba $(Ti_{1-x}\ Zr_x)\ O_3$ (x=0.0, 0.20, 0.40) ceramics were prepared by a sol-gel method. The films were prepared by well established spin coating process. The detailed technique and it relevant theory is given. The effect of Zr content in grain size and room temperature dielectric properties of BZT ceramics were examined and discussed.

2 Spin Coating Technique and Its Theory

The schematic diagram of the spin coating unit is shown in Fig. 1. The physics of spin coating can be effectively modeled by dividing whole process into three stages: deposition and spin up, spin off and film drying, During first stage, solution is allowed to fall on a rotating substrate from micro syringe and the substrate is accelerated to the desired speed. Spreading of the solution takes place due to centrifugal force and height is reduced to critical height. During second stage (spin off), subsequent reduction in film height is dominated by the evaporation of the solvent. During final stage

[1]E-mail: skrout@nitrkl.ac.in

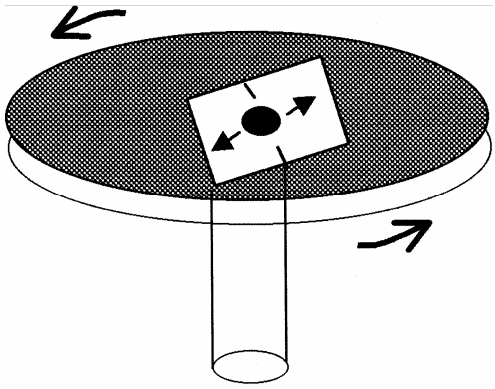

Fig.1 — Schematic diagram of a spin coater

centrifugal outflow stops and further shrinkage is due to solvent loss.

This results in the formation of thin film on the substrate. In actual practice these three stages overlap each other [Yonkoski R K *et al.* 1990)]. The first mathematical model of the spin coating process was given by Emslie (Emslie *et al*. 1958) for a Newtonian fluid. The fluid assumed to be rotating in an infinite plane. Coriolis force and gravitational gradient were neglected. Using cylindrical polar co-ordinates (r, θ, z) with origin at the center of rotation, z perpendicular to the plane, and the axes r and θ rotating with the plane with angular velocity ω, the balance between viscous and centrifugal forces per unit volume for Newtonian fluid is given by:

$$-\eta\left(\frac{d^2v}{dz^2}\right) = \rho\omega^2 r \qquad \ldots (1)$$

where, η is absolute viscosity, ρ the fluid density and v is the velocity in the direction of r.

The radial flow q per unit length of the circumference is given by :

$$q = \int_0^h v(z)dz = (\rho\omega^2 r h^3)/3\eta \qquad \ldots (2)$$

The equation for continuity is given by :

$$r\left(\frac{\partial h}{\partial t}\right) = \frac{\partial (rq)}{\partial r} \qquad \ldots (3)$$

Use of Eqs (2) in (3) yields:

$$\frac{\partial h}{\partial t} = -K\left(\frac{1}{r}\right)\frac{\partial (r^2h^3)}{\partial r}, \text{ where } K = \rho\omega^2/3\eta \qquad \ldots (4)$$

Before seeking general solution of Eq. (4) let us consider the special solution, which depends only on time t. if the distribution of solution is uniform at the beginning, from Eq. (4), we can get:

$$\frac{dh}{dt} = -2Kh^3 \qquad \ldots (5)$$

Integrating both sides with proper limits i.e. at t=0, $h = h_0$ and at t, h=h_t, we get:

$$h_t = h_0/\left(1+4h_0^2Kt\right)^{1/2} = h_0/\left(1+4h_0^2\rho\omega^2 t/3\eta\right)^{1/2} \qquad \ldots (6)$$

Meyerhofer developed a spin model using the equation of continuity for a Newtonian fluid but allowed to the solvent to evaporate during spinning process. He (Meyerhofer D, 1978) approximated that the height of the fluid h could be separated into the height of the solid S and the height of the solvent L i.e h=S+L. By expressing the concentration of the solid $C(t)$ to be C (t) =S/(S+L), one can obtain from the equation of continuity

$$\frac{dS}{dt} = -C(t)\frac{2\omega^2h^3}{3\vartheta} \qquad \ldots (7)$$

where ϑ is the kinetic viscosity $\left(=\frac{\eta}{\rho}\right)$. Including the liquid evaporation rate ϕ, the change in liquid height can be expressed as;

$$\frac{dL}{dt} = -\left(1-C(t)\right)\frac{2\omega^2h^3}{3\vartheta} - \varphi \qquad \ldots (8)$$

The viscosities of these solutions has been reported to be the power law function of the concentration which can be written as;

$$\vartheta = \vartheta_L + \vartheta_S C^{\gamma}(t) \qquad \ldots (9)$$

where ϑ_L and ϑ_S are the viscosities of solvent and solid respectively and γ = 2.5. The final film height can be simplified to the form

$$h = \left[\frac{3C^3(t)\vartheta_0\varphi}{2\{1-C_0(t)\}\omega^2}\right]^{1/3} \text{ or } h \propto \omega^{-2/3} \qquad \ldots (10)$$

where ϑ and $C(t)$ are approximated to be equal to ϑ_0 and $C_0(t)$ i.e the initial viscosity and the initial concentration, respectively.

3 Experimental Details

Precursor solution of $Ba(Zr_xTi_{1-x})$ O3 (x=0.0, 0.2, 0.4 as starting material) was synthesized from barium acetate, zirconium n-propoxide and titanium isopropoxide. Stoichiometric amount of barium acetate was dissolved in warm acetic acid through continuous stirring. Ethylene glycol was added to the solution for complete dissolution of barium acetate in acetic acid. Inside a moisture-controlled glove box, stoichiometric amount of titanium isopropoxide and zirconium n-propoxide was co-dissolved and chelated with acetic acid. Finally, the Zr-Ti complex sol was added drop wise to barium acetate solution at room temperature through continuous stirring to get the desired composition. The compositions were diluted to a concentration of 0.35 mol/lit with the addition of acetic acid. Thin films were prepared on platinised silicon wafer by spin coating technique using a Milman spin coater. The films were deposited at a spinning speed of 3000 rpm for 5 min. Just after deposition, the films were fired at 600°C for 5 min for organic removal and crystallization into perovskite phase. The coating and fairing sequence was repeated 20 times to attain films approximately 800 nm thick. Finally, these were annealed at 1100°C for 2h for perovskite phase formation and improvement in crystallinity. The phase formation behaviour and surface morphology of these films were analyzed by X-ray diffraction. The surface morphology and film thickness were studied by SEM. For electrical measurement, a gold electrode of 400 μm square was deposited on the top of the film by *dc* supttering. The substrate platinum was used as bottom electrode. The room temperature frequency dependence of permittivity and loss tangent was studied by HP 4192A low frequency impedance analyzer.

4 Results and Discussion

Figure 2 shows the room temperature XRD plot of x=0.0, 20.0 and 40.0 atom % Zr substitution in $BaTiO_3$ thin films. All the films were crystallized in to single phase perovskite structure(Fig.2) . Substitution of Ti by higher radii Zr increases the *d* spacing yielding the shift of diffraction peaks towards lower angle. This is a clear indication that Zr is systematically dissolved in $BaTiO_3$ lattice in the studied composition range. As reported in the bulk studies, depending upon Zr content BZT may have tetragonal, orthorhombic, rhombohedral or cubic structure at room temperature. In the present paper, all the compositions are indexed as cubic by comparing with standard pattern for $Ba(Ti_{0.75}Zr_{0.25})$ O_3 (PDF No. 36-0019) . The identification of this phase is not very precise in all compositions because of the close proximity of the diffraction angle of these phases.

Figure 3 shows that SEM micrograph of sol gel derived BZT thin film platinised silicon wafer. All the films were subjected to a final anneal to 1100°C.The average crystalline of pure $BaTiO_3$ film is found to be less then 10nm.The addition of Zr to the $BaTiO_3$ lattice decreased the grain size of the crystallized films. The decreasing grain size with increasing zirconium may be attributable to lower grain growth rates from the slower diffusion of the Zr^{4+} ion, which has a bigger ionic radius than Ti^{4+}. Crystallization may be initiated earlier with lower zirconium

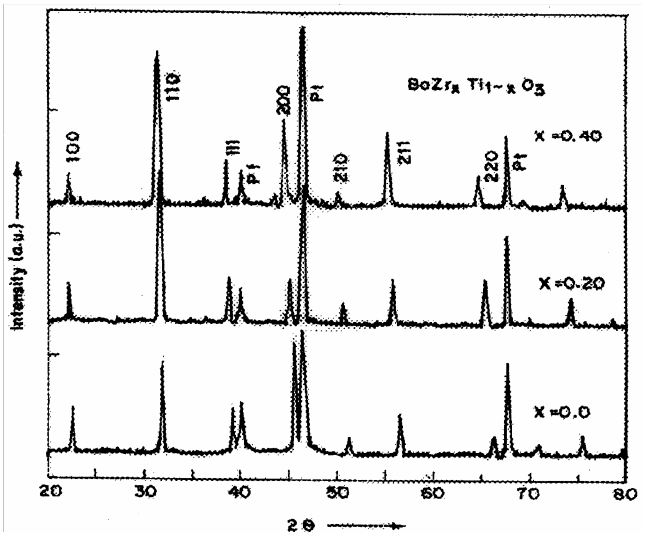

Fig. 2 — X-ray diffraction pattern of $BaTi_{1-x}Zr_xO_3$ thin film with various Zr contents

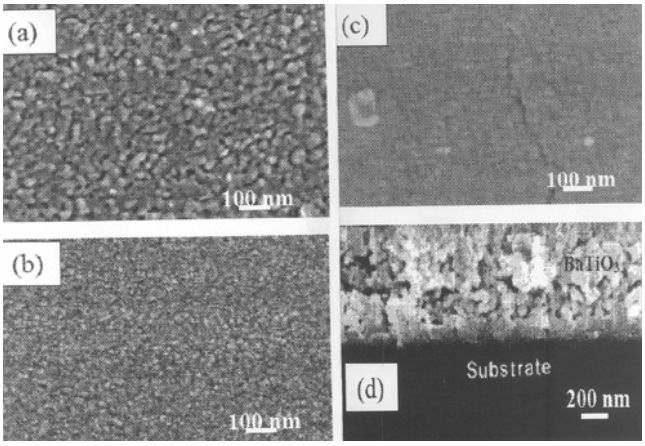

Fig. 3 — SEM micrograph of sol-gel deposited (a) Surface morphology $BaTiO_3$ (b) Surface morphology $BaTi_{0.8}Zr_{0.2}O_3$ (c) Surface morphology $BaTi_{0.6}Zr_{0.4}O_3$ and (d) Cross sectional view of $BaTiO_3$ thin film, after final annealing at 1100°C

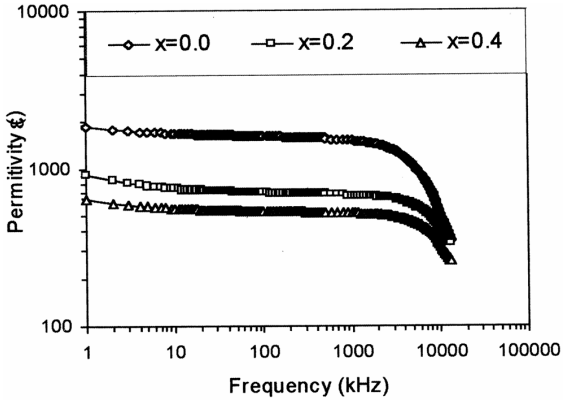

Fig.4 — Frequency dependency of permittivity of different $Ba(Ti_{1-x}Zr_x)\ O_3$ compositions

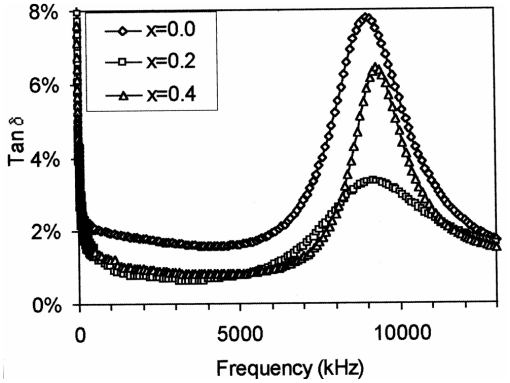

Fig. 5 — Frequency dependency of dielectric loss of different $Ba(Ti_{1-x}Zr_x)\ O_3$ compositions

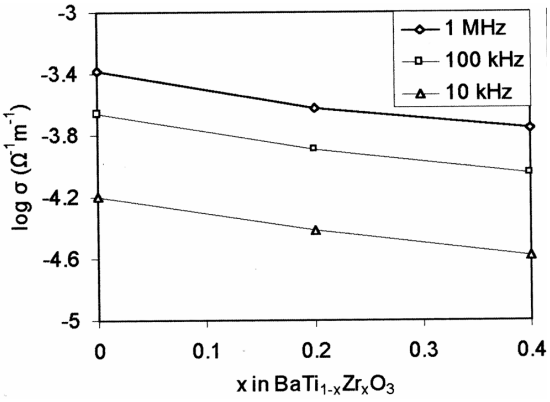

Fig. 6 — Variation of *ac* conductivity with Zr (*x*) content in $Ba(Zr_xTi_{1-x})\ O_3$ ceramics

contents, resulting in a larger grain size for the same heat treatment [11].

Figure 4 shows the frequency dependency permittivity of $BaTi_{1-x}Zr_xO_3$ compositions. Permittivity of all the compositions was very stable in the frequency range 1 kHz to about 8 MHz. In general, permittivity (ε) decreases with the increase in Zr substitution due to; (i) decrease in concentration of high permittivity material $BaTiO_3$ (ii) decrease in grain size resulting in the decrease in polarizability of the atoms in the structure. So it may be concluded from the study that the materials are suitable for application in the frequency range 1 kHz to about 8 MHz.

Figure 5 shows the frequency dependency of the dielectric loss of the samples. In general, δ decreases with Zr-substitution. At very low frequency, high dielectric loss is observed due to the presence of all types of polarization including space charge polarization. That also quickly decreases up to about 1MHz due to the decrease in space charge polarization. The dielectric loss of all the compositions was very stable in the frequency range 1 kHz to about 8 MHz and this loss is within two per cent indicating the good quality of the materials as well as the thin film. At high frequency, a dielectric loss peak is observed. Several possible causes exist for such dispersion including the hypothesis of the influence of the contact resistance between the prob and electrode, resonance due to high dielectric constant. Similar frequency dispersion behaviour was also reported for other ferroelectric thin film [12-14].

For through analysis of the electrical properties, conductivity (σ) of the samples were calculated using the formula $\sigma = 2\pi fCd\ \tan\delta/A$. Where f is the operating frequency, d the thickness of the film, A the area of the electrode, tanδ the dielectric loss and C is the capacitance. The variation of *ac* conductivity with Zr content in the ceramic is plotted in Fig. 6. The conductivity was found to decrease with increase in Zr concentration and frequency. As suggested by Astala[15], impurities and defects are considered to have largest effect in titanate ceramics. i.e higher the defect higher will be the conductivity. Here, as Zr addition reduces the defects in the ceramic that may be the reason for decrease in conductivity with substitution.

5 Conclusions

It may be concluded that (1) Zr is systematically dissolves in $BaTiO_3$ lattice in the studied composition range; (2) diffusion of Zr is relatively slower than Ti due to its higher ionic radii, resulting in lower grain growth in the samples; (3) permittivity of all the compositions was very stable in the frequency range 1 kHz to about 8 MHz. The permittivity (ε) decreases with the increase in Zr substitution due the decrease in polarizability of the atoms in the structure; (4) tanδ decreases with Zr-substitution; (5) dielectric

conductivity decreases with Zr-substitution due to the decrease in charge defects by the substitution, decrease in grain size resulted due to increase in number of grain boundaries per unit thickness.

References

1 Tagantsev A K, Sherman V O, Astafiev K F, Venkatesh J & Setter N, J *Electroceramics*, 11 (2003) 5.

2 Zhi Y, Chen A, Guo R & Bhalla A S, *Appl Phys Lett,* 81 (2002) 1285.

3 Ravez J, Broustera C & Simon A, *J Mater Chem*, 9 (1999) 1609.

4 Tang X G, Chan H L & Ding A L, *Thin Solid Films*, 460 (2004) 227.

5 Zhi Y, Chen A, Guo R & Bhalla A S, *J Appl Phys*, 92 (2002) 2655.

6 Weber U, Greuel G, Boettger U, Weber S, Hennings D & Waser R, *J Am Ceram Soc*, 84 (2001) 759.

7 Tang X G, Chan H L W & Ding A L, *Thin Solid Films,* 460 (2004) 227.

8 Sciau Ph, Calvarin G & Ravez J, *Solid State Commun*, 113 (2000) 77.

9 Homann S & Waser R, *J Euro Ceram Soc*, 19 (1999) 1339.

10 Hennings D, Schnell A & Simon G, *J Am Ceram Soc,* 65 (1982) 539.

11 Farhi R, Marssi M E, Simon A & Ravez J, *Eur Phys J B: Cond Matter Phys*, 9 (1999) 599.

12 Gust M C, Momoda L A, Evans N D & Mecartney M L, *J Am Ceram Soc*, 84 (5) (2001) 1087.

13 Das R R, Bhattacharya P & Katiyar R S, *Appl Phys Lett,* 81 (9) (2002) 1672.

14 Pontes F M, Pontes D S L, Leite E R & Longo E, *J Appl Phys,* 91 (10) (2002) 6650.

15 Astala R K & Bristowe P D, Modelling Simul Mater Sci Eng, 12 (2004) 79.